Pergamon

Journal of Structural Geology, Vol. 20, No. 11, pp. 1435 to 1448, 1998

PII: S0191-8141(98)00047-9

0191-8141/98 $ - see front matter

Deformation mechanisms in the mylonite/ultramylonite transition

J. F. HIPPERTT

Departamento de Geologia, Universidade Federal de Ouro Preto, 35400-000, Ouro Preto, MG, Brazil

and

F. D. HONGN

CONICET, Facultad de Ciencias Naturales, Universidad Nacional de Salta, Buenos Aires 177, 4400 Salta, Argentina

(*Received* 19 *June* 1997; *accepted in revised form* 1 *May* 1998)

Abstract—The deformation mechanisms and controls that operate in the mylonite/ultramylonite transition are interpreted from microstructural observation. The investigated mylonites and ultramylonites were derived from a granitic protolith which was deformed under greenschist facies conditions, and in the presence of fluid, in a regional-scale shear zone from northwest Argentina. Several deformation mechanisms were recognized to operate simultaneously in different domains of the microstructure at each particular stage of the microstructural evolution. This continuously mobile deformation partitioning, present throughout the microstructural evolution, ceases abruptly in the ultramylonite stage, where a stable-state microstructure is achieved. Domainal quartz *c*-axis fabrics indicate that quartz deforms by crystal-plastic processes at the initial and intermediate stages of deformation, but solution-transfer processes become predominant in the ultramylonite stage. Plagioclase is progressively transformed into muscovite through retrograde softening reactions. K-feldspar is progressively transformed into fine-grade aggregates via cataclastic flow and incipient recrystallization. Mica deforms by kinking and basal slip, with progressive development of fine-grained, morphologically oriented aggregates. Plagioclase disappearance as well as the development of intrafolial microfolds characterize the transition between the mylonitic and ultramylonitic domains. Disruption of these microfolds is interpreted to represent the ultimate control on the localization of the ultramylonite bands. © 1998 Elsevier Science Ltd. All rights reserved

INTRODUCTION

Ultramylonites (Quensel, 1916) are tectonites formed in high strain domains of some shear zones which have developed under low and medium metamorphic grade conditions. In ultramylonites, the grain size of the recrystallized matrix is typically smaller than 10–20 μm, and the porphyroclasts are generally rounded due to rotation and development of recrystallized tails. Currently, the use of the term 'ultramylonite' is commonly restricted to tectonites where the volume of relic porphyroclasts is smaller than 10%. Ultramylonites are also commonly enriched in phyllosilicates, so some authors refer to them as phyllonites. Ultramylonites occur most commonly as well-defined millimeter to centimeter-scale bands that pass laterally into mylonites, the transition zone between the two domains being generally quite abrupt. The factors that control the localization of the ultramylonite bands, however, are still poorly understood. Current hypotheses generally invoke heterogeneities in the protolith and/or the presence of pre-existing fractures (e.g. Goodwin and Wenk, 1995) as the main controls on the localization of ultramylonite bands.

This paper investigates the deformation mechanisms and controls that operate in the mylonite/ultramylonite transition, using as an example a granitic mylonite formed in the regional-scale, low metamorphic grade (greenschist facies) Agua Rosada shear zone of northwest Argentina. This shear zone was chosen because it contains, both at hand-specimen and thin section scales, well-defined mylonite and ultramylonite domains separated by a narrow transition zone where the deformation mechanisms responsible for this microstructural transformation could be investigated. This paper principally addresses the deformation processes and controls that operate in the transition zone. XRF whole-rock analyses of major elements in representative samples of mylonite, ultramylonite and precursor granite are also provided. The composition of the different feldspar varieties was determined through EDS microprobe analyses. X-ray diffractometry was used to identify the phyllosilicate minerals as well as to determine the structural state of K-feldspar.

GEOLOGICAL SETTING

The mylonite zone described in this paper crops out in the Agua Rosada gulch near the town of Angastaco in northwest Argentina (Fig. 1). This region consists of Neoproterozoic–Lower Cambrian, low–medium grade

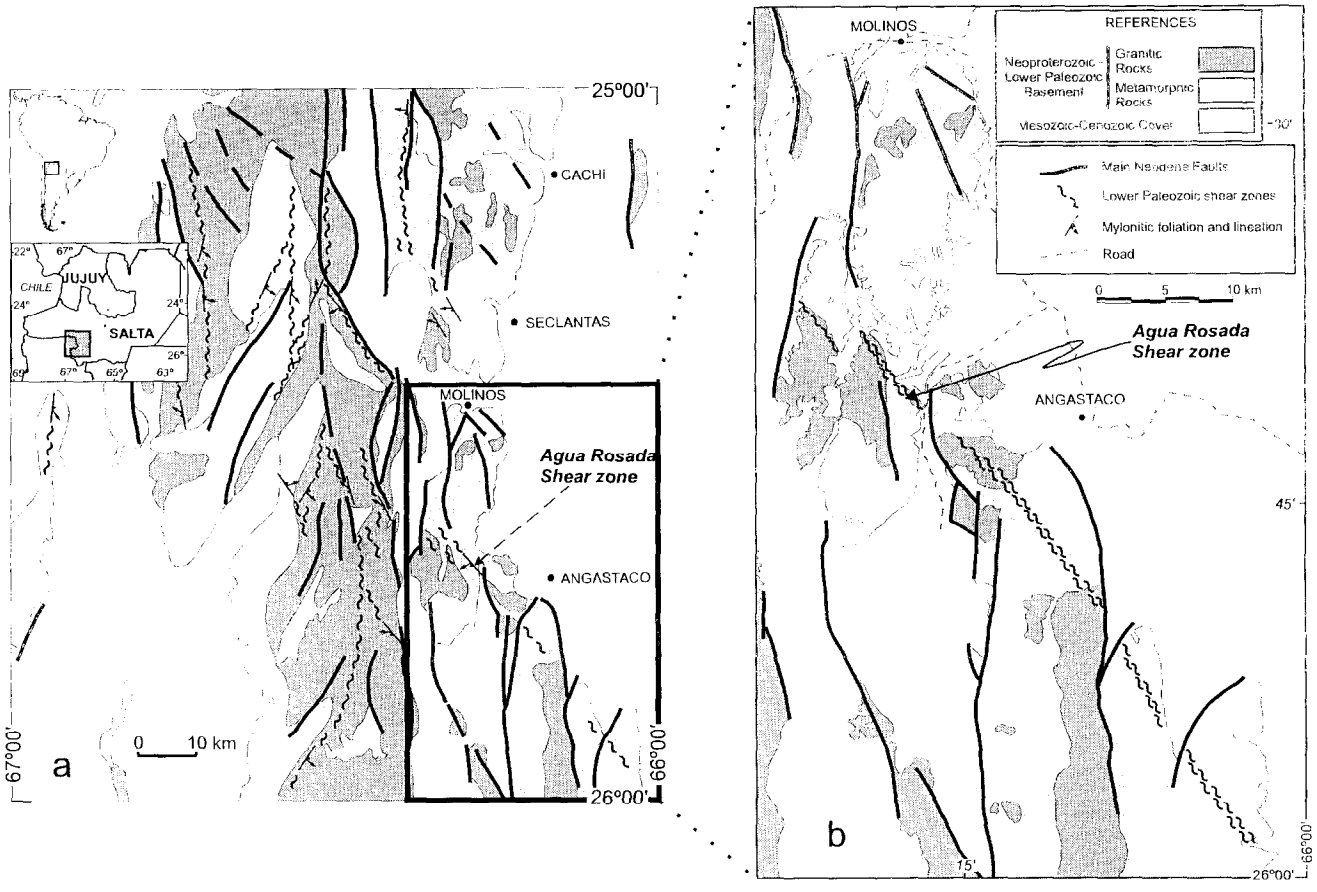

Fig. 1. Simplified geological map showing the location of the Agua Rosada shear zone in northwest Argentina.

metamorphic rocks intruded by Lower Paleozoic granites (Lork *et al.*, 1989). The Agua Rosada shear zone is part of a regional system of mylonite zones developed in the granitic basement of northwest Argentina (LeCorre and Rosello, 1994; Mon and Hongn, 1996). These mylonite zones show different kinematics and are tentatively interpreted as conjugate shears related to a transpressional tectonic regime associated with the Caledonian orogenesis in South America (Hongn *et al.*, 1996). The Agua Rosada shear zone strikes N45° W and dips approximately 75° SW. A dip-slip movement is indicated by a stretching mineral lineation plunging around 65–75° SW.

The Agua Rosada shear zone extends for about 35 km with an average width of 500 m, being truncated in several places by recent Neogene faults (Fig. 1). This shear zone affects both the metamorphic rocks and granitic rocks of the region, the more strongly developed deformational fabrics occurring in the granitic rocks. Within the sheared granitic rocks, it is possible to separate three lateral domains according to their kinematics and the distribution of tectonite types. The central domain (350 m-wide on average) consists of 10–100 m-wide zones of protomylonites or undeformed granite separated by well-defined, 1–5 m-wide mylonitic–ultramylonitic belts. All kinematic indicators (rotated porphyroclasts, *S–C* structures, oblique shape fabrics in recrystallized quartz aggregates, etc.) consistently indicate a normal sense of shear for the high strain bands of this central domain. The external domains are between 30 and 50 m wide and consist principally of homogeneous mylonite with minor proportions of millimetric/centimetric ultramylonite bands whose microstructures indicate a reverse sense of movement (thrusting). This paper deals only with the tectonites produced in the central part. The kinematic variations across this shear zone are not addressed here, but may be related to the bulk strain partitioning in a local transpressional regime.

The high strain deformation zones consist of typical mylonites and ultramylonites. Within these deformation zones, mylonites are widely predominant (> 90% volume) and are characterized by the presence of pinkish feldspar-rich bands (0.2–1 cm wide) developed via fracturing and stretching of the original K-feldspar megacrysts, alternating with quartz-rich and mica-rich bands. Ultramylonites appear in outcrop and hand specimens (Fig. 2) as sharp, homogeneous bands of fine-grained material (width varying from a few millimeters to some decimeters) being easily identified by their color (light gray or green) which contrasts with the coarser grain size and pinkish color of the adjacent mylonitic domains.

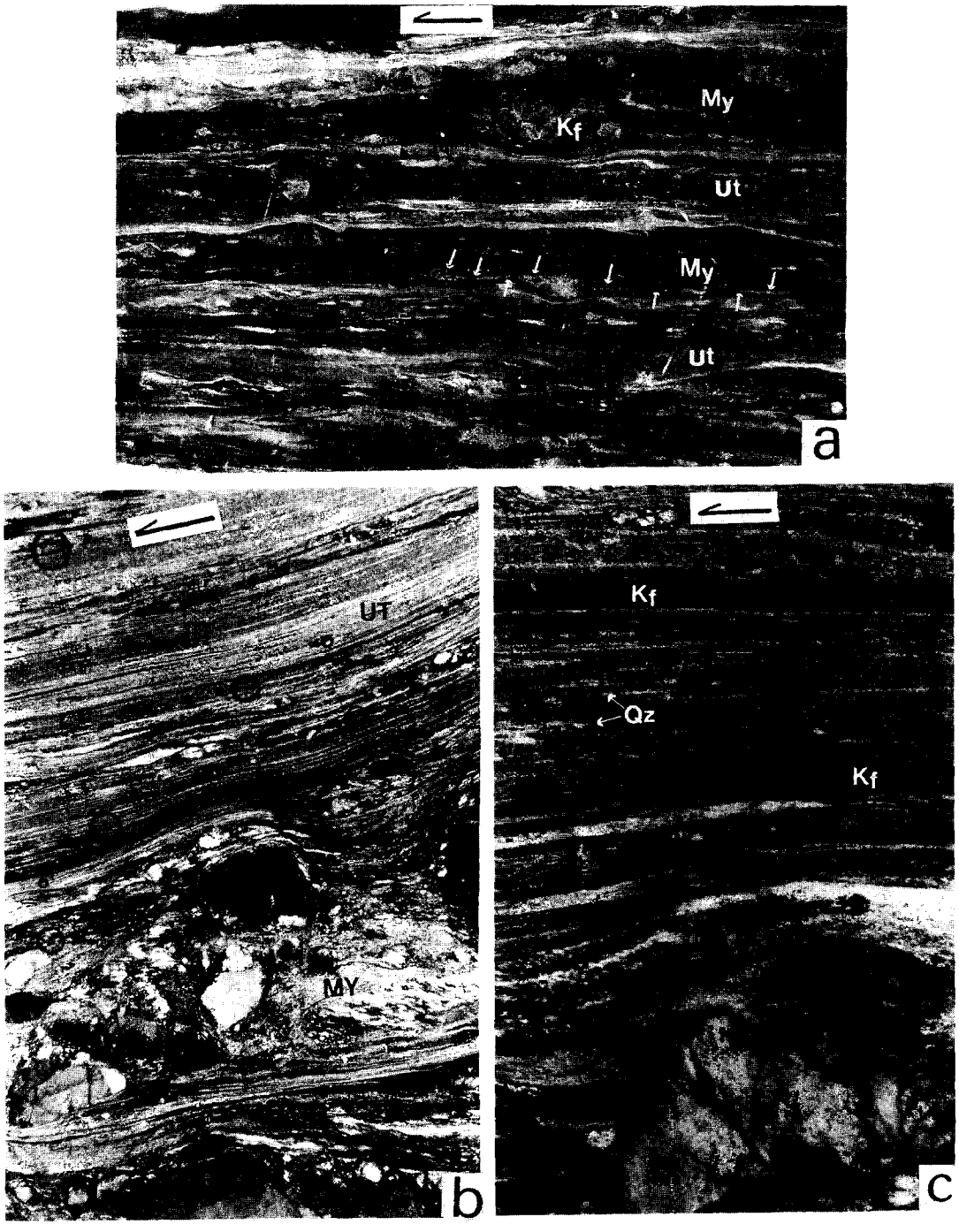

Fig. 2. Mylonitic and ultramylonitic bands observed at different scales. (a) Alternating mylonitic (My) and ultramylonitic (Ut) bands in a polished hand specimen. Note the disruption and spreading of the K-feldspar fragments forming pure K-feldspar bands (arrows). Width of view 8 cm. (b) Photomicrograph showing the abrupt contact between a mylonitic band (My) and an ultramylonitic band (Ut). K-feldspar fragments occur as porphyroclasts in the mylonitic band. Width of view 2.8 mm. Crossed polarizers. (c) Detail of a mica-rich ultramylonitic band containing internal K-feldspar rich layers (K_f) and thin quartz ribbons (Qz). Note the curved contact close to a K-feldspar porphyroclast of an adjacent mylonitic band in the bottom of the photograph. Width of view 0.45 mm. Crossed polarizers.

Within the central part of the Agua Rosada shear zone, deformation is very heterogeneous and shows a remarkable strain partitioning at all scales. Mylonites and ultramylonites occur in well-defined, high strain deformation zones contiguous to domains of protomylonites and undeformed granite. A complete transition between undeformed protolith and mylonite is generally observed in a zone a few decimeters-wide. The undeformed rock is a coarse-grained, pink-red granite with up to 4 cm-long misoriented K-feldspar megacrysts (microcline; bulk composition $Or_{90\text{-}98}Ab_{10\text{-}2}An_{<0.3}$), and mica contents around 15% (biotite and muscovite in equal proportions). Grain size of the original micas varies from 1 to 4 mm.

Plagioclase ($Ab_{83-75}An_{15-25}Or_{<2}$) occurs in equidimensional grains (0.2–0.6 mm). Plagioclase content is about 30%.

The Agua Rosada shear zone was developed in a strain path close to ideal simple shear, as indicated by the asymmetry of single girdle *c*-axis fabrics in quartz (cf. Lister and Hobbs, 1980; Law, 1990; Law *et al.*, 1990) and monoclinic symmetry in porphyroclast systems (Passchier and Simpson, 1986). Metamorphic conditions were within the greenschist facies ($T < 450$°C) as indicated by the presence of syn-deformational muscovite, predominant brittle and reaction-assisted deformation of feldspars (FitzGerald and Stünitz, 1993) and crystal-plastic deformation of quartz via single slip on basal ⟨*a*⟩ glide (cf. Lister and Williams, 1979). Evidence for fluid activity during shearing includes the production of muscovite via reaction-softening in feldspar (White and Knipe, 1978; Dixon and Williams, 1983), and chloritization–muscovitization of the original biotite. The presence of very fine chlorite aggregates along grain boundaries of the weakly deformed protomylonite indicates that fluid circulation occurred since the earliest stages of deformation.

DESCRIPTION OF THE MICROSTRUCTURE

On the microscale, both mylonite and ultramylonite display a well-defined planar fabric (*C*-foliation) and a mineral stretching lineation marked by the alignment of mica crystals and ribbon quartz. Both mylonite and ultramylonite present a tectonic banding consisting of bands of different composition, hence with different rheologic properties. The transition between the mylonitic and ultramylonitic domains occurs in narrow zones (< 0.5 mm thick) which present a banding with intermediate characteristics between mylonite and ultramylonite. The microstructure of these three domains (Fig. 3) is described in detail below.

Mylonite

The mylonite microstructure consists of poorly defined bands of disrupted K-feldspar megacrysts forming typical domino-like microstructures wrapped by dynamically recrystallized pure quartz layers lacking porphyroclasts. The K-feldspar fragments (0.2–2 cm) are angular, their shape being generally controlled by cleavage planes. Incipient tails of fine-grained K-feldspar ($Or_{95-99}Ab_{5-1}An_{<0.1}$) can be found in the strain shadows adjacent to some fragments. Flame and vein perthites ($Ab_{93-78}An_{5-12}Or_{<3}$) occur along grain margins and fractures. The large original mica crystals (biotite and muscovite) are kinked and disrupted to form fine-grained, mica-rich bands. X-ray diffractometry of a representative mylonite sample detected the presence of muscovite, paragonite and minor amounts of biotite and chlorite as the main phyllosilicates present. All original quartz is segregated in finely recrystallized (grain size 10–30 μm), pure quartz bands. The recrystallized quartz aggregates show strong crystallographic preferred orientation (CPO) with a *c*-axis maximum oriented at a low angle to the foliation pole (Fig. 4). Plagioclase occurs as non-fractured crystals which are generally surrounded by a mantle of fine-grained white mica (muscovite-paragonite) (Fig. 5b). Typical mantled porphyroclast systems are sometimes formed. The mica aggregates of the porphyroclast mantles are progressively stretched to form incipient pure mica bands. The global mylonitic microstructure can be visualized as an alternating sequence of three types of bands: (1) K-feldspar + quartz, (2) pure quartz, and (3) plagioclase + mica bands. Apart from the partial transformation of both plagioclase and original mica into very fine mica, no other modal changes in relation to the undeformed protolith were observed. The mylonite is significantly enriched in Mn, P and H_2O and depleted in Fe, Mg and Ti relative to the protolith rock, a tendency that is strengthened towards the ultramylonite stage (Fig. 6).

Ultramylonite

The most noticeable characteristic of the ultramylonite microstructure is its low content of quartz and plagioclase. The well-defined quartz layers of the mylonite nearly disappear in the ultramylonite bands. Close to the margins, however, the ultramylonites contain fine relics of quartz aggregates with the same CPO as the mylonitic domains. In the interior of the ultramylonite bands, however, only very fine monocrystalline quartz grains occur. These grains show a *c*-axis preferential orientation with a maximum at a low angle to the lineation (Fig. 4), which contrasts radically with the CPO of the mylonites (maximum close to the foliation pole). Plagioclase also is nearly absent in most bands. In contrast, the white mica content (product of plagioclase breakdown) increases dramatically in the ultramylonites in the form of fine-grained aggregates. K-feldspar occurs as stretched layers of finely crushed microbreccia (microcline, $Or_{97-99}Ab_{3-1}An_{<0.2}$) where a few, rounded porphyroclasts can be seen. Muscovite and paragonite are the only phyllosilicates present. The global ultramylonitic microstructure consists essentially of three types of alternating bands: (1) pure mica bands, (2) pure K-feldspar bands (fine-grained aggregates plus porphyroclasts) and, (3) quartz + mica bands. Profound differences in the modal composition exist in relation to the protolith rock, suggesting that significant mass transfer processes accompanied the ultramylonite formation, which is also corroborated by the diagram of normalized concentration shown in Fig. 6.

Although the relative abundance of elements in the different tectonite types, in itself, does not clarify the

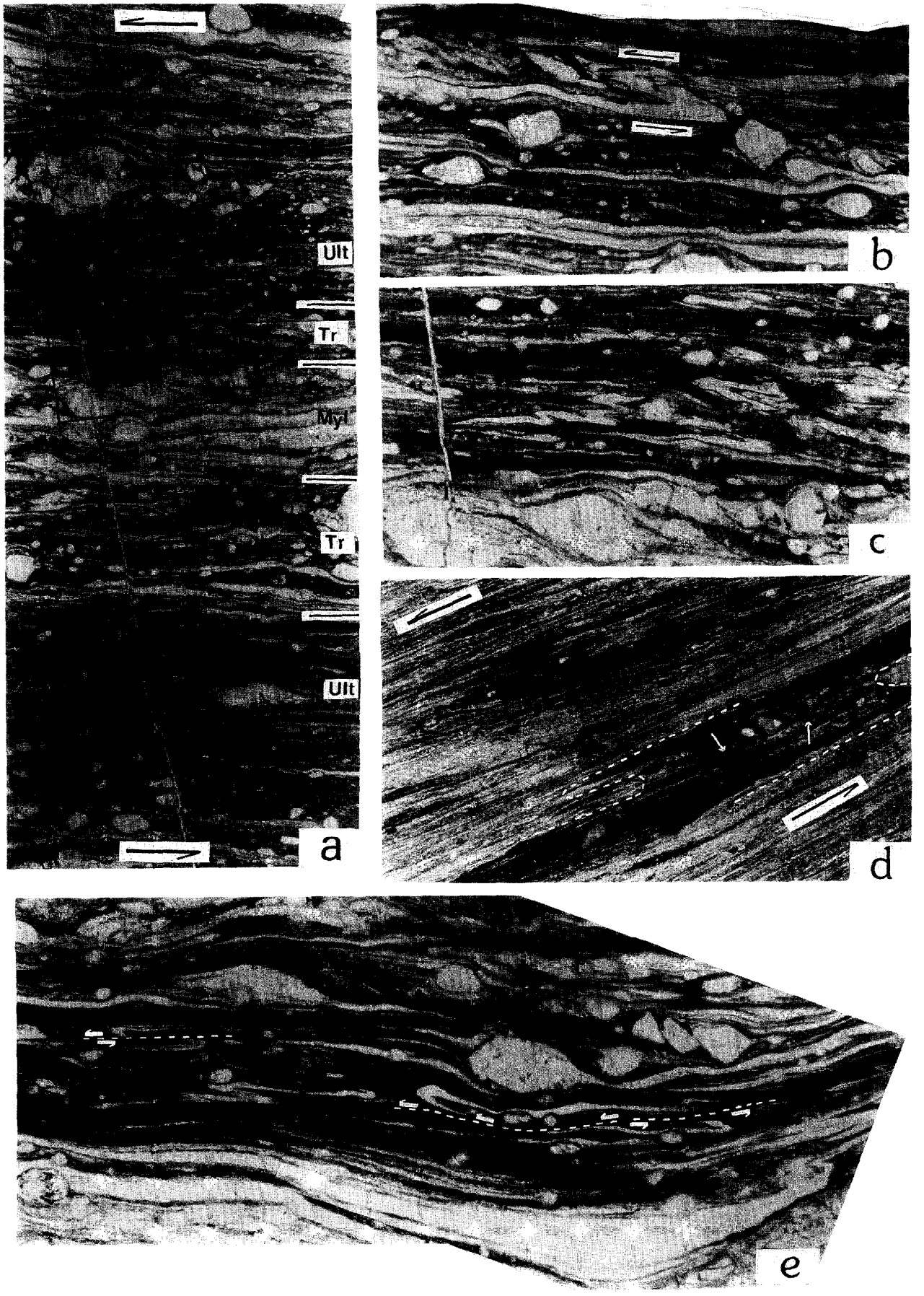

Fig. 3 (*caption overleaf*)

exact degree of mass transfer involved during allochemical deformation/metamorphism (see Ague, 1994), it reflects generally well the main mineralogical transformations that accompanied deformation. Thus, the depletion of Fe, Mg, and Ti shown by mylonites and ultramylonites is consistent with the observed biotite and chlorite breakdown, with subsequent migration of these elements out the mylonite–ultramylonite zones. This situation has also been previously documented in other low-grade shear zones (e.g. Winchester and Max, 1984). On the other hand, the enrichment of Mn and P most probably resulted from a residual concentration due to mass-volume loss, as these elements (principally P) may be left behind during mass transfer of more soluble compounds out of the deformation zone (e.g. O'Hara, 1988; Selverstone *et al.*, 1991). The increasing H_2O content towards the ultramylonites is also consistent with the progressive mica enrichment and plagioclase breakdown that accompanied deformation. In contrast, the normalized abundances of Si, Al and alkalis, which are very close to 1, suggest that significant migration of these elements, in or out of the mylonite–ultramylonite zones, probably did not occur.

Transition zone

The transition zone between mylonites and ultramylonites is typically narrower than 0.5 mm. There is a smaller proportion of K-feldspar porphyroclasts (20–30%), which are smaller (0.1–0.5 mm) and tend to be more rounded than in the mylonites. Another difference is the presence of better developed tails of fine-grained K-feldspar in strain shadows of porphyroclasts. Plagioclase is nearly absent. Muscovite–paragonite occurs in fine layers where rare plagioclase relics are found. Quartz occurs as fine-grained, dynamically recrystallized aggregates in pure quartz bands. The global microstructure of the transition zone can be visualized as an alternating sequence of pure K-feldspar bands (consisting of porphyroclasts plus crushed material), pure quartz bands and muscovite–(plagioclase) bands.

The most characteristic feature of the transition zone, however, is the noticeable development of isoclinal microfolds whose asymmetry is consistent with the overall shear sense (Fig. 3). These microfolds have an intrafolial character and are usually defined by inflection of the quartzose bands (and, occasionally, of the K-feldspar bands) between two consecutive mica bands. The fine-grained mica bands are not folded, but disrupt the thinned limbs of some microfolds in domains immediately adjacent to the ultramylonite bands. These microfolds are interpreted to exert a crucial role on the localization of the ultramylonite bands, as discussed below.

DEFORMATION MECHANISMS

The banding of the mylonitic, ultramylonitic and transitional domains reflects rock flow partitioning during shearing, with strain in each individual band being accommodated by one or more specific deformation mechanisms. In this section, based on our microstructural observations, we interpret the different deformation mechanisms for the principal minerals, and discuss the contribution of these mechanisms for the overall rock deformation.

Quartz

In the mylonites, all the quartz is concentrated in pure quartz bands that extend parallel to the shear plane and are not laterally connected to each other. These bands consist of fine-grained recrystallized aggregates with a noticeable oblique grain shape fabric consistent with the overall shear sense and strong crystallographic preferred orientation (CPO) of *c*-axes around the foliation pole. This CPO is commonly attributed to activation of basal ⟨*a*⟩ slip, the glide system of quartz with lower activation energy at low metamorphic grade conditions (Hobbs, 1985), whose operation rotated the basal planes to progressively lower angles to the overall shear plane. Lack of *c*-axes close to *Y*-axis of finite strain, or between the *Y*- and *Z*-axes of strain also indicates that prism and rhomb ⟨*a*⟩ glide (also possible glide systems at low grade conditions) were not operative (Schmid and Casey, 1986) and that quartz was deformed and segregated in bands via single slip on the basal ⟨*a*⟩ glide system. Even in sites of flow perturbation such as those occurring around porphyroclasts or microfolds, the ductile flow of the quartzose layers was accommodated via basal ⟨*a*⟩ slip, as the basal planes of quartz are systematically oriented parallel to the folded surface of the quartzose band (Fig. 4b). The small dimensions of the recrystallized grains, the strong CPO and the oblique grain shape fabric at angles lower than 40° suggest that

Fig. 3. Photomicrographs of microfolds in the mylonite/ultramylonite transition. (a) A mylonitic band (Myl) is enclosed between two ultramylonitic bands (Ult). Microfolds occur in the transition zones (Tr) between the mylonitic and ultramylonitic domains. Parallel polarizers. Width of view 3.2 mm. (b) Folded quartz band consistent with sinistral shear. Note the intrafolial character of the microfold. Parallel polarizers. Width of view 2.4 mm. (c) Detail of the area marked in (a). Several disrupted microfolds and some relic fold hinges are outlined in the photo. Parallel polarizers. Width of view 2.4 mm. (d) Relic fold hinges of K-feldspar bands (dark material) within a mica-rich ultramylonitic band. The arrows indicate thin mica bands that cross-cut the outlined K-feldspar domain. Crossed polarizers. Width of view 1.1 mm. (e) Stretched fold limbs and disrupted microfolds in a domain immediately adjacent to an ultramylonitic band. Parallel polarizers. Width of view 4.0 mm.

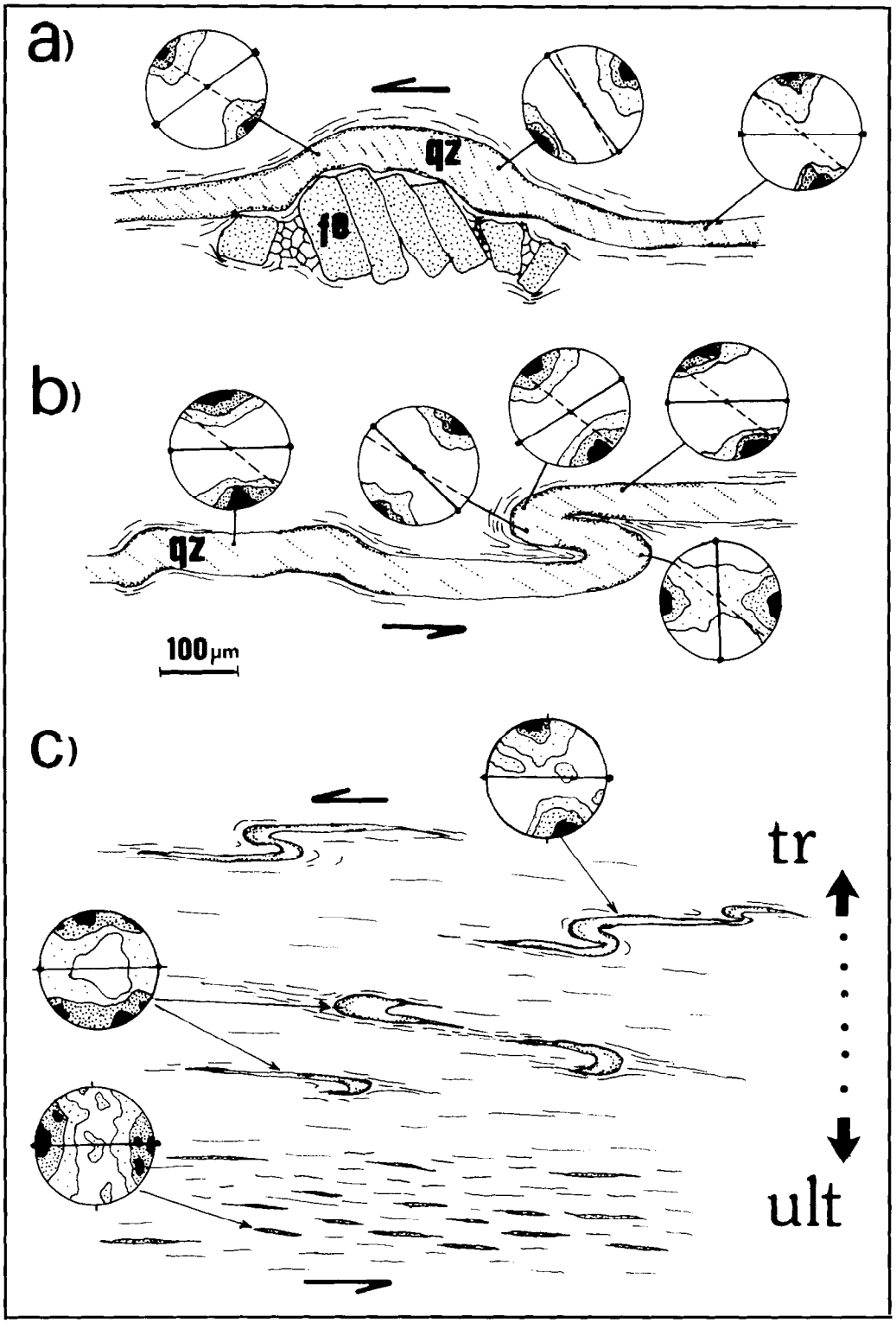

Fig. 4. Representative domainal quartz *c*-axis fabrics in mylonites and ultramylonites. (a) Variation of *c*-axis preferential orientation in a quartz band deflected over a fractured feldspar grain showing a 'domino' microstructure. Orientation of the band boundaries (solid lines) and internal grain shape fabric (dashed lines) are indicated in all stereoplots. Note how the basal planes are systematically oriented parallel to the band boundaries. (b) *c*-Axis preferential orientation along a quartz microfold. There is a complete variation of *c*-axis orientation which reflects the parallelism between basal planes of quartz and the band boundaries all over the microfold. (c) Variation of quartz microstructures and corresponding *c*-axis fabrics in the transition to an ultramylonite zone. In the transition zone (*tr*), folded quartz bands and relic microfold hinges show a *c*-axis preferential orientation at high angles with the flow plane (horizontal lines). In the ultramylonite zone, the thin quartz ribbons show a totally contrasting pattern, where the *c*-axis is preferentially oriented at low angles to the stretching lineation (heavy dots). All sketches were draw from *XZ*-thin sections. Density contours are 1, 4 and 8% per 1% area in all diagrams. $N = 75$ in all diagrams of (a) and (b). $N = 200$ in the three diagrams of (c). All stereoplots are equal angle, lower hemisphere projections.

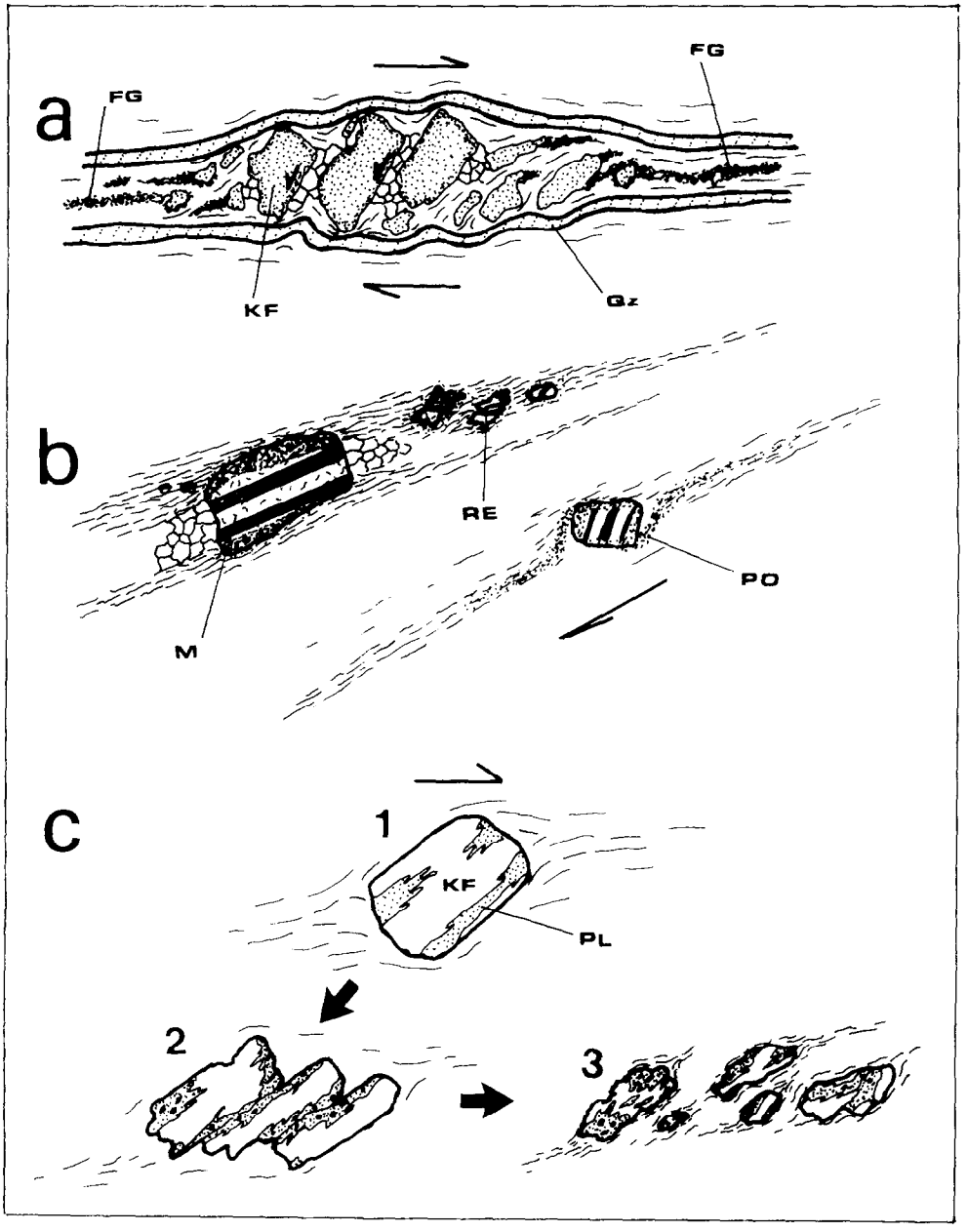

Fig. 5. Deformation microstructures in feldspar grains. (a) Fracture and development of 'domino' microstructures in a K-feldspar-rich band enclosed between two pure quartz bands. Cataclastic flow of the fine grained, crushed K-feldspar (FG) enabled progressive stretching within the K-feldspar layer. (b) Microstructures indicative of plagioclase breakdown through mica-producing softening reactions. Reactions were more intense in the plagioclase margins that are in contact with mica layers (M). Plagioclase relics (RE) show typical irregular, 'corroded' outlines. Muscovite derived from the softening reactions form porphyroclast tails (PO) with δ geometries. (c) Sketch illustrating progressive deformation of K-feldspar in parallel with development of replacement perthites. Stage 1 corresponds to development of replacement perthitic veinlets (stippled) oriented at low angles to the *S*-planes. In stage 2, muscovitization and breakdown of the perthitic plagioclase favors the development of fractures, disrupting the original K-feldspar crystal. Stage 3 illustrates the advanced stage of deformation where feldspar relics with a rounded outline are immersed in a muscovite-rich matrix.

recrystallization was syn-kinematic (i.e. dynamic; cf. Urai *et al.*, 1986), and that a relatively high shear strain (cf. Ramsay and Graham, 1970) was accommodated in the quartzose layers. Such features are not consistent with static recrystallization because this process, apart from promoting grain growth and weakening deformational crystallographic fabrics, generally destroys pre-existing oblique grain shape fabrics. Lack of quartz porphyroclasts and the extreme stretching of the individual, non-connected quartzose bands (aspect ratio > 30) also suggest that these bands, as well as the mica-rich bands (see below), acted as preferential flow planes in the evolving mylonitic microstructure. Even in the K-feldspar-bearing bands, stretching of the original K-feldspar megacrysts via fracturing and spreading of fragments was ultimately accommodated by

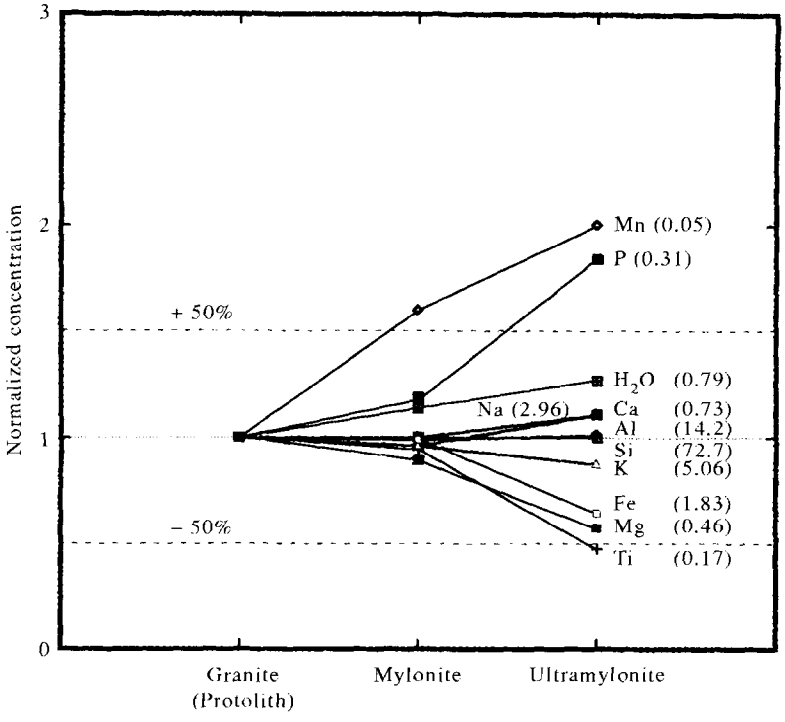

Fig. 6. Diagram showing the major element content of mylonites and ultramylonites from the Agua Rosada shear zone normalized by the composition of the protolith granite. Numbers between parentheses indicate the oxide content (in %) of each major element in the protolith.

plastic deformation of the quartz films (finely recrystallized and with strong CPO) that anastomose around the individual K-feldspar fragments (Figs 4a & 5a).

In contrast, the quartz content decreases abruptly in the ultramylonites. Domainal quartz *c*-axis fabrics in the thin ribbons of the ultramylonite bands revealed the presence of maxima at low angles to the stretching lineation (*X*-maximum) (Fig. 4c). Similar CPOs were found in quartz aggregates deformed by solution-reprecipitation creep at low metamorphic grade conditions (e.g. Hippertt, 1994; Takeshita and Hara, 1998), and have been interpreted as being indicative of solution-transfer processes. During solution-reprecipitation creep in quartz aggregates, the development of CPO is attributed to anisotropic growth/dissolution rates on different crystallographic directions of quartz, the faster rates occurring along the ⟨*c*⟩ direction (Tullis, 1989). Thus, grains oriented with *c*-axis at low angles to the maximum extension direction of finite strain are expected to grow faster (or dissolve more slowly) than those at high angles, leading to the development of *c*-axis maxima at low angles to the stretching lineation. Alternatively, this CPO could be interpreted as a result of crystal-plasticity through activation of prism ⟨*c*⟩ slip (e.g. Bouchez *et al.*, 1984). However, activation of prism ⟨*c*⟩ glide has been documented only in rocks deformed at temperatures higher than 650–700°C (Mainprice *et al.*, 1986; Garbutt and Teyssier, 1991), making this hypothesis unlikely in this shear zone. Evidence for activity of an aqueous fluid and consequent quartz solution-transfer is also given by the noticeable mica enrichment in the ultramylonite bands. In turn, the mica enrichment may also enhance fluid circulation in the ultramylonite bands as the rock permeability generally increases in the presence of morphologically oriented mica crystals (see Bell and Cuff, 1989). Another possible control on the increasing contribution of solution transfer in the ultramylonite bands is exerted by the finer grain size of quartz in these domains, as the efficiency of solution-transfer has been inferred to be inversely proportional to d^3, where d is grain size (Shimizu, 1995).

The transition zone shows a different character of quartz deformation marked by intrafolial folding of the quartz bands. The quartz grains are always oriented with basal planes parallel to the folded surface, indicating that basal ⟨*a*⟩ slip also operated during fold development. The presence of these intrafolial folds in the transition zone may reflect a sharp gradient in the local strain rate between the rheologically different bands of the transition zone, and suggests that ductile stretching of the quartzose bands was not sufficient to accommodate progressive strain in the transition zone, leading to the observed microfolding.

Mica

The role of micas is very important in both the initial and advanced stages of progressive deformation. The proportions of biotite and muscovite are roughly

the same in the undeformed or weakly deformed granites. In these domains, the original mica crystals show different behaviors according to their orientation relative to the shear plane. Mica grains oriented at right angles to the foliation (*C*-planes) are strongly kinked while those at low angles to the foliation show curved or disrupted (001) basal surfaces. Fine-grained chlorite aggregates are observed along the incipient foliation planes defined by mica, suggesting that these foliation surfaces were a locus of fluid activity. This fluid activity probably favored the softening reactions that produced very fine white mica from the original plagioclase in the mylonitic/ultramylonitic domains.

Muscovite was more resistant to deformation than biotite. In the initial stages of deformation, retrograde reactions in the presence of an aqueous fluid promoted the complete transformation of biotite into chlorite and fine-grained muscovite. Some original muscovite is preserved in the form of porphyroclasts and mica fish (Lister and Snoke, 1984). The newly formed chlorite, however, disappears in the high strain mylonitic/ultramylonitic domains, probably in response to the migration of Mg, Fe and Ti out these deformation zones (Fig. 6).

The mica-producing softening reactions in plagioclase were more intense on grain boundaries that are in contact with mica-rich bands, confirming that fluid circulation probably took place along the micaceous bands. This mechanism (Fig. 5b) allowed very fine white mica to be aggregated to the mica bands. In these mica bands, the mica grains are preferentially oriented with basal planes parallel to the mylonitic foliation and, therefore, in a position of easy slip for mica. Therefore, all these sequential processes appear to constitute a feed-back mechanism that progressively increased strain accommodation in the mica bands. With progressive deformation, the mica bands became pervasive due to plagioclase disappearance and connection between adjacent mica bands.

Feldspar

In the mylonitic domains, K-feldspar deformed principally via fracturing along crystallographic cleavage planes forming large, angular porphyroclasts. The incipient recrystallization adjacent to some fractures and along grain margins indicates that deformation conditions were close to the brittle-ductile transition for K-feldspar (Simpson, 1985). With progressive strain, mantles and tails of fine-grained feldspar (5–15 μm) are formed. These aggregates are composed of equidimensional polygonal grains, but do not show any optically visible crystallographic orientation. These features suggest that these aggregates may correspond to gouge zones that were subsequently recrystallized (Tullis *et al.*, 1990), although this is difficult to assess by optical means.

Another important feature is the development of flame and vein perthites in the K-feldspar porphyroclasts. These perthites are restricted to the deformed granitoids and their development has a direct relationship with disappearance of the matrix plagioclase due to the mica-producing softening reactions. The perthitic plagioclase occurs principally in flames and veinlets along grain margins occupying sometimes 50–60% of the volume of the original K-feldspar grain, a proportion that does not correspond to the Ab content (2–10%) of the original K-feldspar. In addition, there is no apparent crystallographic control on the distribution of the perthitic plagioclase as typically occurs in exsolution perthites. All these features are consistent with an origin via external replacement (replacement perthites, cf. Pryer and Robin, 1996).

Replacement perthites are common in granitoids deformed under low grade conditions in the presence of aqueous fluid, where plagioclase is transformed into muscovite through softening reactions. In these reactions, Ca and Na are released from the reacting plagioclase and may either migrate out of the system (e.g. Selverstone *et al.*, 1991) or, in some shear zones, be used to form epidote (e.g. O'Hara, 1988). Another possibility is that some of the Ca^{++} and Na^{+} ions, isostructurally replace K^{+} in the K-feldspar forming replacement perthites. In turn, the K^{+} ions released from the K-feldspar are used to form muscovite (Hippertt, 1998), as the K-feldspar is the main source for potassium in these rocks. This process should be more effective after biotite disappearance, as a new source for K is necessary to continue the plagioclase breakdown through mica-producing softening reactions. So the overall process is interpreted as a combination of two reactions operating simultaneously, i.e. muscovitization of plagioclase, and development of replacement perthites by isostructural ionic exchange of alkalis (Hippertt, 1998). These reactions account for all the observed transformations without any external access of elements. Subsequent muscovitization of the perthitic plagioclase also contributes to continued disruption and grain size reduction of the K-feldspar megacrysts (Fig. 5c). The process should advance until all of the plagioclase in the rock is consumed.

Figure 6 shows that there is no apparent alkali depletion with progressive strain, suggesting that paragonite (a Na-bearing phyllosilicate) should have acted as the main sink for Na after plagioclase disappearance. However, a sink for the relatively low Ca content in these rocks (< 1%) is not obvious, as epidote, the most common Ca-bearing mineral produced by retrograde reactions in granitic rocks, is not present in the studied mylonites and ultramylonites. Apart from that, the K-feldspar (both from porphyroclasts and fine-grained aggregates) is also nearly Ca-free. Thus, solid solution of Ca replacing K and Na in the structure of muscovite paragonite appears as the most likely sink for Ca in these tectonites.

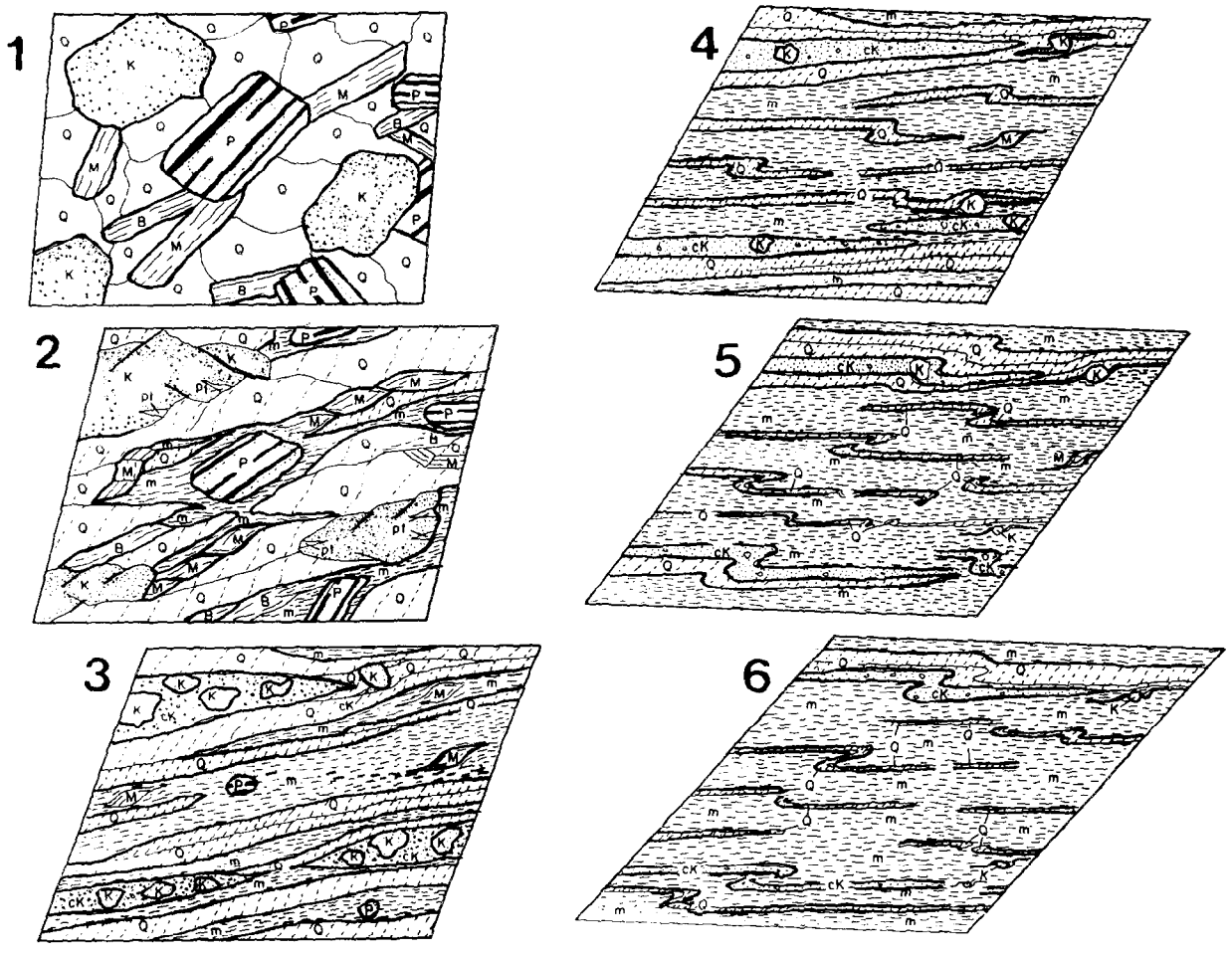

Fig. 7. Sketch illustrating the evolving microstructure of the sheared granitoid. Stage 1: Granitic protolith with K-feldspar (K), zoned plagioclase (P), muscovite (M), biotite (B) and quartz (Q). In Stage 2, quartz is plastically segregated into pure quartz bands which define an incipient banding. Mica deforms by kinking and fracturing. Typical mica fishes are formed. Plagioclase is partially transformed into muscovite along grain margins. Fractures, pull-aparts and microshears occur in K-feldspar grains. Stage 3 shows an intensification of the tectonic banding. Fine-grained, K-feldspar bands develop from original K-feldspar megacrysts by fracturing and cataclastic flow. Rounded plagioclase relics occur in small proportions in bands of fine-grained muscovite. Stage 4 represents the disappearance of plagioclase and enhanced strain accommodation in the mica bands causing microfolding of the quartz bands. K-feldspar is nearly totally transformed into a fine-grained aggregate by cataclastic flow. Stages 5 and 6 show the progressive closure and disruption of the microfolds.

Breakdown of plagioclase generally begins along grain margins and cleavage planes where access of fluid enables the mica-forming reactions to proceed. Fracture was not an important deformation mechanism in plagioclase, and evidence for crystal-plasticity was not observed. With the progressive reaction and the consequent disappearance of plagioclase, pure mica bands are formed, with preferentially oriented mica flakes acquiring an orientation of easy slip on basal planes of mica, consequently decreasing the bulk strength of the rock (Shea and Kronenberg, 1993). Disappearance of plagioclase, therefore, should represent a major change in the rheology and resulting deformation partitioning. In the presence of decreasing amounts of quartz, these pure mica layers appear to have become the main strain accommodator, consequently controlling the localization of the ultramylonitic bands.

DISCUSSION

Mylonite/ultramylonite transition—the role of microfolding

Based on the observed microstructures we suggest that the progressive deformation of a protolith granitoid into ultramylonite (Fig. 7) is marked by three major kinks in the strain–time path (Fig. 8). These kinks are interpreted to correspond to significant

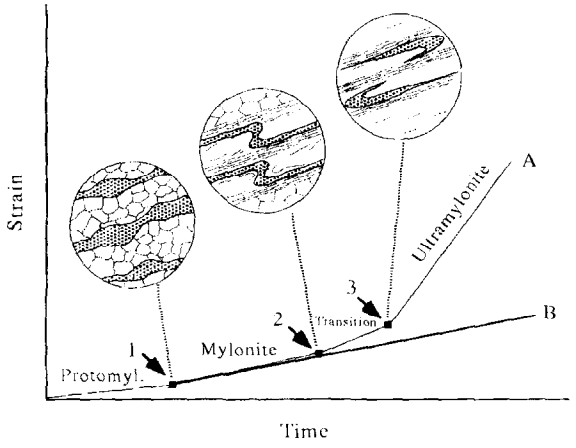

Fig. 8. Suggested kinked strain–time path for progressive deformation of granitic rocks with development of high-strain, ultramylonitic zones (path A). Major changes in the microstructure cause abrupt increases in the strain accommodation (softening) during progressive deformation. Plastic segregation of quartz and development of folia characterize the beginning of the mylonitic microstructure. The next kink in the strain path corresponds to the disappearance of plagioclase and development of pure mica bands. These pure mica bands become the weakest layers in the microstructure, thus accommodating most of the strain and inducing microfolding of the adjacent pure quartz bands. The next kink marks the beginning of the ultramylonitic microstructure and is characterized by disruption of the quartz microfolds and pervasive development of mica folia. Strain path 'B' represents the development of a mylonite where softening mechanisms and strain localization in ultramylonite zones did not occur.

changes in the microstructural evolution due to abrupt alterations in the contributions of the different deformation mechanisms. The first kink occurs when interconnection of the weakest phase (quartz) leads to formation of ribbons, enhancing strain accommodation (and strain localization) via intracrystalline slip in the quartz bands. This kink characterizes the transition from a protomylonite to a mylonite with a well-defined planar fabric. The development of these well-defined flow planes favors the development of a tectonic banding in the mylonite microstructure, which should represent the energetically most economic configuration regarding the rheology of the different minerals and the operative deformation mechanisms in each stage of the microstructural evolution. Thus, bands of crushed/recrystallized K-feldspar and bands of plagioclase-mica are also formed in parallel with quartz ribboning. All these bands are continuously stretched via crystal-plastic processes in the quartz bands, grain size reduction and cataclastic flow in the K-feldspar bands, and progressive breakdown of plagioclase in the plagioclase–mica bands.

The second major kink occurs when the breakdown of plagioclase through the mica-producing softening reactions is complete and plagioclase disappears. Thus, the obstacles that might block the tectonic flow in the mica layers are eliminated, allowing interconnection of the morphologically oriented mica crystals and greater strain accommodation via basal slip of mica. In fact, after disappearance of the plagioclase, the pure mica bands seem to become the weakest domain of the mylonitic microstructure, where the strong rheological contrasts with the quartz bands and K-feldspar bands cause the observed microfolding. Development of these microfolds characterizes the transition zone that occurs between the mylonitic and ultramylonitic domains.

In the transition zone, deformation leads to progressive closure of the microfolds in parallel with progressive stretching of the fold limbs towards the ultramylonite domains. The third kink in the strain path corresponds to the disruption of the fold limbs, causing a pervasiveness of the mica folia and consequent increase in strain accommodation. This kink marks the first appearance of typical ultramylonitic microstructures and is interpreted to represent the ultimate control on the localization of the ultramylonitic bands.

Intrafolial microfolding is also an effective way to imbricate the micaceous bands leading to a progressively finer banding and consequent homogenization of the microstructure, a main characteristic of ultramylonites. In the ultramylonites, the remnant fold hinges of the quartz and feldspar layers are further stretched to form thin lenses of quartz and feldspar surrounded by a micaceous matrix. It is suggested that the fine banding increases the relative surface/volume ratio of the quartz bands enhancing continued quartz dissolution with resultant mica-enrichment in the ultramylonite domains.

CONCLUSIONS

1. Under low metamorphic grade conditions and in the presence of an aqueous fluid, progressive deformation of granitoids occurs through many different deformation mechanisms operating in different microstructural domains at each particular stage of the fabric evolution.
2. The deformation partitioning continuously changes during the progressive evolution from a granitic protolith to an ultramylonite. In the protomylonite and mylonite stages, deformation of quartz is accommodated by crystal-plastic processes. However, these processes decrease in importance in the ultramylonite stages where solution-transfer is predominant. Plagioclase is deformed via mica-producing softening reactions. After plagioclase disappearance, pure mica bands are formed and slip on basal planes of mica appears to become the most important deformation mechanism. K-feldspar deforms predominantly by fracturing, cataclastic flow and incipient crystal-plasticity. No changes in the deformation mechanisms of K-feldspar are observed with progressive strain.

3. Major changes in the deformation partitioning correspond to drastic changes in the microstructural evolution. These changes are interpreted to represent three major kinks in the strain-time path of a deforming granitic rock. The first kink occurs when interconnection of the weakest phase (quartz) is attained, forming ribbons and starting the development of a tectonic banding. This kink marks the transition from protomylonitic to mylonitic microstructures. The second kink occurs when plagioclase breakdown is complete and pure mica layers are formed. In this stage, strong local strain-rate contrasts between the pure mica bands and quartz/feldspar bands may explain the formation of intrafolial microfolds. The third kink corresponds to a disruption of the microfold limbs causing a pervasiveness of the mica bands. This kink characterizes the beginning of the ultramylonitic stage.

Acknowledgements—Financial support for this research was provided by CIUNSa, CONICET and Argentina National Geological Survey grants to Hongn; and a CNPq research grant (process 533688/96-2) to Hippertt. Steve Matthews made an initial review of the manuscript. Official reviews by G. Godard and an anonymous referee, and an editorial review by R. Norris helped to improve the final version.

REFERENCES

Ague, J. (1994) Mass transfer during Barrovian metamorphism of pelites, south-central Connecticut. I. Evidence for changes in composition and volume. *American Journal of Science* **294,** 989–1057.

Bell, T. and Cuff, C. (1989) Dissolution, solution transfer, diffusion versus fluid flow and volume loss during deformation/metamorphism. *Journal of Metamorphic Geology* **7,** 425–447.

Bouchez, J.-L., Mainprice, D. H., Trepied, L. and Doukhan, J. C. (1984) Secondary lineation in a high-*T* quartzite (Galicia, Spain): an explanation for an abnormal fabric. *Journal of Structural Geology* **6,** 159–165.

Dixon, J. and Williams, G. (1983) Reaction softening in mylonites from the Arnaboll thrust, Sutherland. *Scottish Journal of Geology* **19,** 157–168.

FitzGerald, J. and Stunitz, H. (1993) Deformation of granitoids at low metamorphic grade. I: Reactions and grain size reduction. *Tectonophysics* **221,** 269–297.

Garbutt, J. M. and Teyssier, C. (1991) Prism ⟨*c*⟩ slip in the quartzites of the Oakhurst Mylonite Belt, California. *Journal of Structural Geology* **13,** 657–666.

Goodwin, L. and Wenk, H.-R. (1995) Development of phyllonite from granodiorite: Mechanisms of grain-size reduction in the Santa Rosa mylonite zone, California. *Journal of Structural Geology* **17,** 689–708.

Hippertt, J. F. (1994) Microstructures and *c*-axis fabrics indicative of quartz dissolution in sheared quartzites and phyllonites. *Tectonophysics* **229,** 141–163.

Hippertt, J. F. (1998) Breakdown of feldspar, volume gain and lateral mass transfer during mylonitization of granitoid in a low metamorphic grade shear zone. *Journal of Structural Geology* **20,** 175–193.

Hobbs, B. E. (1985) The geological significance of microfabric analysis. In *Preferred Orientation in Deformed Metals and Rocks: and Introduction to Modern Texture Analysis*, ed. H.-R. Wenk, pp. 463 484. Academic Press, Orlando.

Hongn, F. D., Mon, R., Cuevas, J. and Tubia, J. M. (1996) Zones de cisaillement calédoniennes à haute température dans la Quebrada Barranquilla (Puna Orientale, Argentine); données structurales et cinématiques. *Comptus Rendus Académie de Sciences de Paris, Série IIa* **323,** 809–815.

Law, R. D. (1990) Crystallographic fabrics: a selective review of their applications to research in structural geology. In *Deformation mechanisms, rheology and tectonics*, eds R. Knipe and E. Rutter, pp. 335–352. Geological Society of London, Special Publication **54**.

Law, R. D., Schmid, S. M. and Wheeler, J. (1990) Simple shear deformation and quartz crystallographic fabrics: a possible natural example from the Torridon area of NW Scotland. *Journal of Structural Geology* **12,** 29–45.

LeCorre, C. A. and Rosello, E. (1994) Kinematics of early Paleozoic ductile deformation in the basement of NW Argentina. *Journal of South American Earth Sciences* **7,** 301–308.

Lister, G. S. and Hobbs, B. E. (1980) The simulation of fabric development during plastic deformation and its application to quartzite: the influence of deformation history. *Journal of Structural Geology* **2,** 355–370.

Lister, G. S. and Williams, P. F. (1979) Fabric development in shear zones: theoretical controls and observed phenomena. *Journal of Structural Geology* **1,** 283–297.

Lister, G. S. and Snoke, A. W. (1984) *S-C* mylonites. *Journal of Structural Geology* **6,** 617–638.

Lork, A., Miller, H. and Kramm, U. (1989) U–Pb zircon and monazite ages of the La Angostura granite and the orogenic hystory of the northwest Argentina basement. *Journal of South American Earth Sciences* **2,** 147–153.

Mainprice, D., Bouchez, J. L., Blumenfeld, Ph. and Tubia, J. M. (1986) Dominant *c* slip in naturally deformed quartz: Implications for dramatic plastic softening at high temperature. *Geology* **14,** 819–822.

Mon, R. and Hongn, F. D. (1996) Estructura del basamento proterozoico y paleozoico inferior del norte argentino. *Revista de la Asociacion Geologica Argentina* **51,** 1–10.

O'Hara, K. (1988) Fluid flow and volume loss during phyllonitization—an origin for phyllonite in an overthrust setting, North Carolina, USA. *Tectonophysics* **156,** 21–36.

Passchier, C. W. and Simpson, C. (1986) Porphyroclast systems as kinematic indicators. *Journal of Structural Geology* **8,** 831–844.

Pryer, L. and Robin, P.-Y. (1996) Differential stress control on the growth and orientation of flame perthite: a paleostress-direction indicator. *Journal of Structural Geology* **18,** 1151–1166.

Quensel, P. (1916) Zur Kenntnis der Mylonitbildung erläutert an Material aus dem Kebnekaisegebiet. *Uppsala Universitet, Geologiska Institut Bulletin* **15,** 91–116.

Ramsay, J. and Graham, R. (1970) Strain variation in shear belts. *Canadian Journal of Earth Sciences* **7,** 786–813.

Schmid, S. M. and Casey, M. (1986) Complete fabric analysis of some commonly observed quartz *c*-axis patterns. In *Mineral and Rock Deformation: Laboratory Studies*, eds B. Hobbs and H. Heard. American Geophysical Union, Geophysical Monograph. **36,** pp. 263–286.

Selverstone, J., Morteani, G. and Staude, J.-M. (1991) Fluid channeling during ductile shearing: transformation of granodiorite into aluminous schist in Tauern Window, Eastern Alps. *Journal of Metamorphic Geology* **9,** 419–431.

Shea, W., Jr and Kronenberg, A. (1993) Strength and anisotropy of foliated rocks with varied mica contents. *Journal of Structural Geology* **15,** 1097–1122.

Shimizu, I. (1995) Kinetics of pressure solution creep in quartz: theoretical considerations. *Tectonophysics* **245,** 121–134.

Simpson, C. (1985) Deformation of granitic rocks across the brittle–ductile transition. *Journal of Structural Geology* **7,** 503–511.

Takeshita, T. and Hara, I. (1998) *c*-Axis fabrics and microstructures in a recrystallized quartz vein deformed under fluid-rich greenschist conditions. *Journal of Structural Geology* **20,** 417–431.

Tullis, T. E. (1989) Development of preferred orientation due to anisotropic dissolution/growth rates during solution transfer creep. *Eos, Transactions of the American Geophysical Union* **70,** 457.

Tullis, J., Dell'Angelo, L. and Yund, R. (1990) Ductile shear zones from brittle precursors in feldspathic rocks: the role of dynamic recrystallization. *American Geophysical Union, Geophysical Monograph* **56,** 67–81.

Urai, J. L., Means, W. D. and Lister, G. S. (1986) Dynamic recrystallization of minerals. In *Mineral and Rock Deformation: Laboratory Studies*, eds B. Hobbs and H. Heard. American Geophysical Union, Geophysical Monograph. **36,** pp. 61–99.

White, S. H. and Knipe, R. J. (1978) Transformation- and reaction-enhanced ductility in rocks. *Journal of the Geological Society of London* **135,** 513–516.

Winchester, J. and Max, M. (1984) Element mobility associated with syn-metamorphic shear zones near Scotchport, NW Mayo, Ireland. *Journal of Metamorphic Geology* **2,** 1–11.